JOURNAL OF MATERIALS SCIENCE 28 (1993) 6761–6766

Microstructure and properties of the sintered composite prepared by hot pressing of TiN-coated alumina powder

H. ITOH, H. SUGIMOTO, H. IWAHARA
Synthetic Crystal Research Laboratory, School of Engineering, Nagoya University, Chikusa-ku, Nagoya 464-01, Japan

J. OTSUKA, S. IIO
Research and Development Centre, NGK Spark Plug Co. Ltd, 2808 Iwasaki, Komaki-shi, Aichi 485, Japan

Alumina powders (average grain size: 50 μm) coated with TiN film of thickness 0.5 and 1.2 μm were prepared by rotary powder-bed chemical vapour deposition for 15 and 90 min, respectively. These Al_2O_3–TiN composite powders were hot-pressed at 1800 °C and 40 MPa for 30 min. The microstructure of the Al_2O_3 –TiN sintered composite was composed of a TiN network homogeneously distributed on the grain boundaries of alumina. The mechanical properties (hardness, bending strength and fractured toughness) and thermal conductivity of the sintered composite were found to depend on the composition and microstructure of the sintered composite, even with a small content (3–7 wt%) of TiN. The resistivity of the sintered composite was 10^{-1}–10^{-3} Ω cm. The relatively high electrical conductivity of the Al_2O_3–TiN composite was caused by the grain boundary conduction of TiN.

1. Introduction

Alumina (α-Al_2O_3) based sintered composites containing non-oxide ceramics such as TiC [1–3] and SiC [4, 5] are known to improve the mechanical properties on account of the effects of depressing abnormal grain growth and increasing the toughness of the composite by crack deflection. Other unique thermal and electrical properties of the composite may be derived from its characteristic microstructure. Electrically conductive alumina-based ceramics can be fabricated, for instance, by sintering alumina powder coated with a small content of a non-oxide conducting film such as transition metal nitride, carbide or boride. Kimura *et al.* [6] measured the resistivity of a hot-pressed Al_2O_3–TiN (12.5 wt %) composite obtained by floating-type fluidized-bed chemical vapour deposition (CVD) of alumina powder (grain size: 0.63 μm) and reported a resistivity of 7.5×10^{-1} Ω cm. Table I shows the structural features and properties of pure α-Al_2O_3 and titanium nitride (TiN); alumina is a typical electrical insulator, while TiN has a low resistivity (2.2×10^{-5} Ω cm) similar to that of most transition metals.

We have developed a new procedure for preparing coated composite powders [7–10] by rotary powder-bed CVD (RPB-CVD). Uniform coating of titanium nitride on to iron powder [7, 8] or alumina powder [10] was carried out successfully. It is interesting to investigate what kind of microstructure and properties would emerge from a composite prepared by sintering the coated powders. In the present paper, Al_2O_3 powder coated with a thin film of TiN was hot-pressed under optimum sintering conditions. The mechanical, thermal and electrical properties of the sintered composite were evaluated in relation to its microstructure.

TABLE I Structure and properties of α-Al_2O_3 and TiN

	α-Al_2O_3	TiN
Crystal system	Hexagonal	Cubic
Crystal structure	α-Al_2O_3 type	NaCl type
Density (g cm^{-3})	3.97	5.43
Melting Point (°C)	2050	2950
Microhardness (H_V)	2300	1700
Elastic modulus (GPa)	400	250
Thermal expansion coefficient (K^{-1})	8.1×10^{-6}	9.8×10^{-6}
Thermal conductivity (W m^{-1} K^{-1})	33.5	66.9
Resistivity (Ω cm)	10^{14}	2.2×10^{-5}

2. Experimental procedure

2.1. Preparation of Al_2O_3–TiN sintered composite

Fig. 1 shows the procedure for preparing coated powder and sintered composite in the Al_2O_3–TiN system. The composite powder was prepared by using the RPB-CVD apparatus described in previous papers [7, 9]. A powder of alumina beads with an average diameter of 50 μm was vacuum-treated at 300 °C for 10 min. Then, an adsorption treatment of the powder

0022–2461

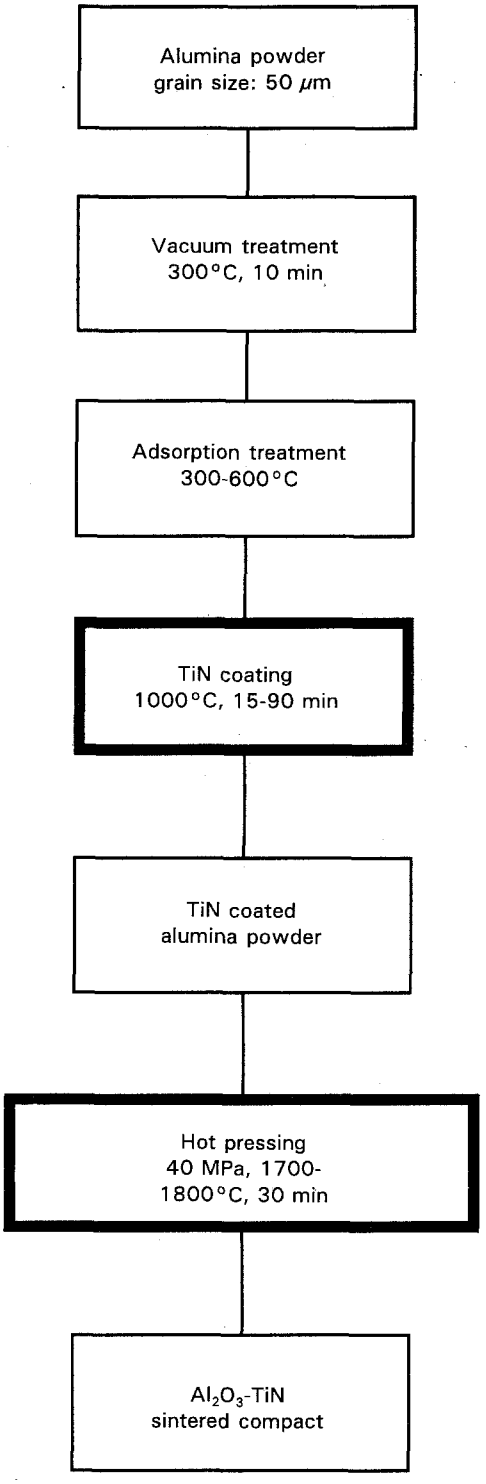

Figure 1 Procedure for preparing coated powder and sintered composite in the Al_2O_3–TiN system.

in a flowing reactant gas ($TiCl_4 + N_2 + H_2$) was carried out during heating from 300 to 600 °C at a heating rate of 15 °C min^{-1} under 760 torr in a specimen cell rotated at 90 r.p.m. The optimum CVD treatment conditions were chosen as follows [10]: rotary speed of specimen cell 90 r.p.m., coating temperature 1000 °C, treatment time 15–90 min, reactant gas flow rates $TiCl_4$ 5 ml min^{-1}, N_2 200 ml min^{-1}, H_2 500 ml min^{-1} and Ar 20 ml min^{-1}. The coated powder (about 20 g) was packed into a graphite mould and heat-treated in a nitrogen atmosphere at 40 MPa and 1700–1800 °C for 30 min, using a uniaxial hot-pressing apparatus. The size of sintered compact obtained was 36 mm × 36 mm × 4 mm.

2.2. Characterization of sintered composite and evaluation of the properties

The sintered specimen was identified by X-ray diffraction, and the microstructures of polished surfaces and fractured cross-sections were examined by optical microscopy and scanning electron microscopy, respectively. The bulk density of the sintered composite was measured by Archimedes' method. The Vickers microhardness of the compact was measured under 1 kg load. Young's modulus was measured by an ultrasonic pulse method. The strength was measured by the three-point bending method. The fracture toughness was measured by the single-edge precracked beam (SEPB) method with a span length of 16 mm. The thermal conductivity was measured by a laser flash method at room temperature. The resistivity of the compact was measured by the four-probe method (d.c.) with a span length of 25 mm.

3. Results and discussion

3.1. Optimum conditions for preparation of Al_2O_3–TiN sintered composite

Fig. 2 shows a typical scanning electron micrograph of cross-section of TiN-coated alumina particles obtained by RPB-CVD at 1000 °C for 60 min. The coated particles were embedded in epoxy resin and the cross-sections were polished with diamond paste. Alumina particles are apparently coated homogeneously with a thin film of TiN. The relation between TiN film thickness and CVD treatment time is shown in Fig. 3, where the film thickness is measured by scanning electron microscopy. TiN content is also plotted on the opposite vertical axis, as calculated from the data on TiN film thickness, Al_2O_3 particle diameter and their theoretical densities. A linear relationship can be seen after a treatment time of 15–30 min, which shows that the TiN content of the coated powder can be controlled by the CVD reaction

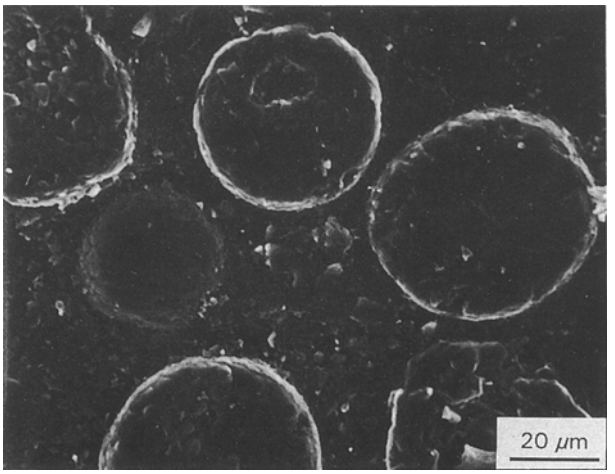

Figure 2 Scanning electron micrograph of cross-sections of TiN-coated alumina particles. CVD treatment temperature 1000 °C, CVD treatment time 60 min.

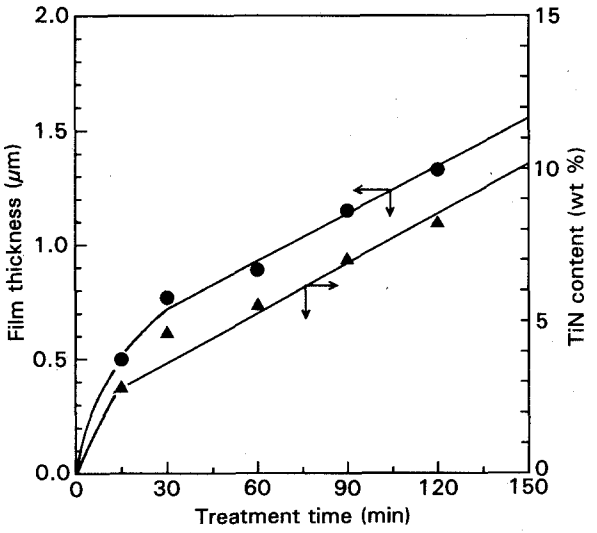

Figure 3 Influence of CVD treatment time on TiN film (●) thickness and (▲) content. CVD treatment temperature 1000 °C.

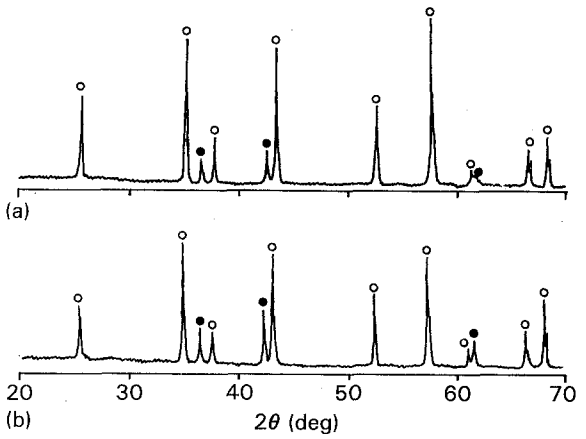

Figure 4 X-ray diffraction patterns (CuK_α) of the surfaces of (a) CVD-15 and (b) CVD-90 specimens. (○) Al_2O_3, (●) TiN; hot pressing temperature 1800 °C, pressure 40 MPa, soaking time 30 min.

time. In the present experiments, the treatment times of 15 and 90 min were chosen in order to examine the effect of the difference in film thickness and TiN content on the microstructure and properties of the sintered composite. The film thickness and TiN content for a reaction time of 15 min are 0.5 μm and 3 wt %, respectively, while those for a reaction time of 90 min are 1.2 μm and 7 wt %, respectively. These two kinds of TiN-coated alumina powder were used as starting powders for hot pressing.

It was found from a series of preliminary hot-pressing experiments that the optimum sintering conditions of temperature and pressure were 1800 °C and 40 MPa, respectively, at a constant soaking time of 30 min. Fig. 4 shows X-ray diffraction patterns of the specimen surfaces obtained under the above optimum hot-pressing conditions. As shown in Fig. 4a, strong diffraction lines for α-Al_2O_3 and weak lines for TiN are identified in the specimen prepared from the alumina powder coated for 15 min (referred to hereafter as the CVD-15 specimen). The intensities of TiN peaks increases in the case of the specimen prepared from the powder coated for 90 min (the CVD-90 specimen, Fig. 4b). No other crystalline phases were detected in either specimen, which verifies that sintered composites in the binary Al_2O_3–TiN system had been prepared.

3.2. Microstructure of Al_2O_3–TiN sintered composite

Fig. 5a–d shows optical micrographs of the polished surfaces of hot-pressed specimens obtained from the two kinds of coated powder. The photographed surface plane is perpendicular to the hot-pressing direction. The white and grey portions correspond to TiN and Al_2O_3, respectively. The TiN network, which is distributed over the whole surface of the specimen, can be seen on the grain boundaries of hot-pressed alumina grains in Fig. 5a and c. The TiN grain-boundary layer thickness of the CVD-15 specimen is thinner than that of the CVD-90 specimen, as presumed from the film thicknesses of the coated powders.

A continuously connected circular pattern of cross-sectioned coated particles appears in a large area of the specimen surface (see magnified pictures in Fig. 5b and d). On the other hand, an abnormal white coloured pattern comprised of TiN thin film can be seen in some places where a hot-pressed TiN layer between alumina particles would appear on the polished specimen surface. The approximate relative density of the composite is estimated from the porosity (black portions on the micrographs) to exceed 95%, which agrees with the relative density calculated from the ratio of bulk to powder densities.

Fig. 6a–f shows back-scattered electron images of the fractured surfaces of CVD-15 (Fig. 6a–c) and CVD-90 specimens (Fig. 6d–f) with various magnifications. The fractured surface is parallel to the hot-pressing direction, which lies in the top to bottom direction of each micrograph. An elliptical cross-sectional pattern of hot-pressed coated particles is seen in Fig. 6a and d. Particle deformation during densification is affected by the hot-pressing direction, as seen by comparing the compressed particle shapes in Figs 5 and 6. Grain growth of alumina is observed within a coated particle. However, an exaggerated grain growth of alumina beyond the TiN grain boundary cannot be seen. Closed pores are located mainly in alumina grains and the densification between alumina particles and the TiN layer looks sufficient. The fracture mode of the specimen seems to be composed of intra-granular fracture and grain boundary fracture, which causes a deflection of crack propagation. However, fractures are seen to occur occasionally penetrating the weak grain boundaries, especially in the CVD-15 specimen.

3.3. Properties of Al_2O_3–TiN sintered composite

Table II summarizes the mechanical, thermal and electrical properties of the sintered composites of

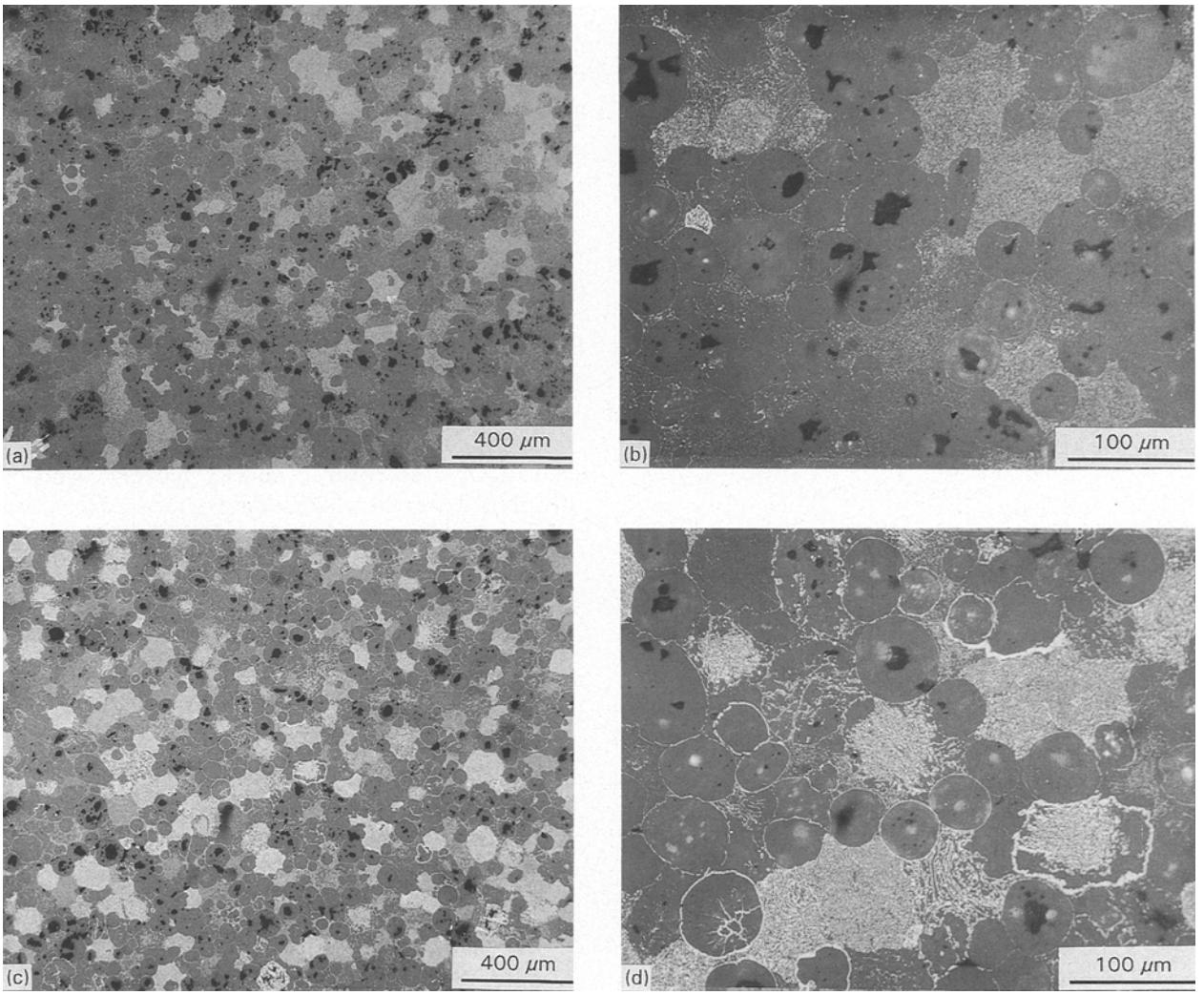

Figure 5 Optical micrographs of the polished surfaces of hot-pressed specimens: (a, b) CVD-15; (c, d) CVD-90; (b, d) magnified micrographs of (a) and (c), respectively.

TABLE II Properties of Al_2O_3–TiN sintered composites

	CVD treatment time	
	15 min	90 min
TiN film thickness (μm)	0.5	1.2
TiN content (wt %)	3	7
Density (g cm^{-3})	3.97	4.07
Microhardness (H_V)	2000	1900
Young's modulus (GPa)	388	382
Bending strength (MPa)	280	280
Fracture toughness (MPa m$^{1/2}$)	4.0	5.2
Thermal conductivity (W m^{-1} K^{-1})	26.6	26.2
Resistivity (Ω cm)	2.0×10^{-1}	2.0×10^{-3}

CVD-15 and CVD-90 specimens, the TiN film thicknesses and contents being also included in the table. The bulk densities of the two specimens were 3.97 and 4.07 g cm^{-3}, respectively, and the relative densities could be estimated in the range of 95–98% from calculation of the ratio of bulk to powder densities measured by Archimedes' method. The average value of Vickers microhardness was 1900–2000 kg mm^{-2}, which was similar to that of a single phase of alumina sintered compact. The indentation volume was smaller than the grain size of alumina, which resulted in less influence of TiN hardness. The Young's modulus (382–388 GPa) of the composite seems to follow the linear rule of mixtures, depending on its Al_2O_3–TiN composition. The bending strength of both specimens was 280 MPa, which was less than values reported for other Al_2O_3-based composites [1, 2, 4, 5]. The fractured toughness increased from 4.0 MPa m$^{1/2}$ in the CVD-15 specimen to 5.2 MPa m$^{1/2}$ in the CVD-90 specimen. The toughness is found to depend on the thickness of the TiN film at the grain boundary (as described in section 3.2). The thermal conductivity of both composites was of the order of 26 W m^{-1} K^{-1}, which was lower than that of single phases of Al_2O_3 and TiN (compare with Table I).

The resistivities of CVD-15 and CVD-90 specimens were respectively 2.0×10^{-1} and 2.0×10^{-3} Ω cm, both specimens being electrical conductors even though the TiN contents are in the low range of 3–7 wt % (2–5 vol %). These conductivities cannot be explained by the percolation theory applied to random mixtures of mechanically mixed Al_2O_3 and TiN [11]. As shown in Fig. 5, the TiN network will contribute to the electrical conduction of the composite. By

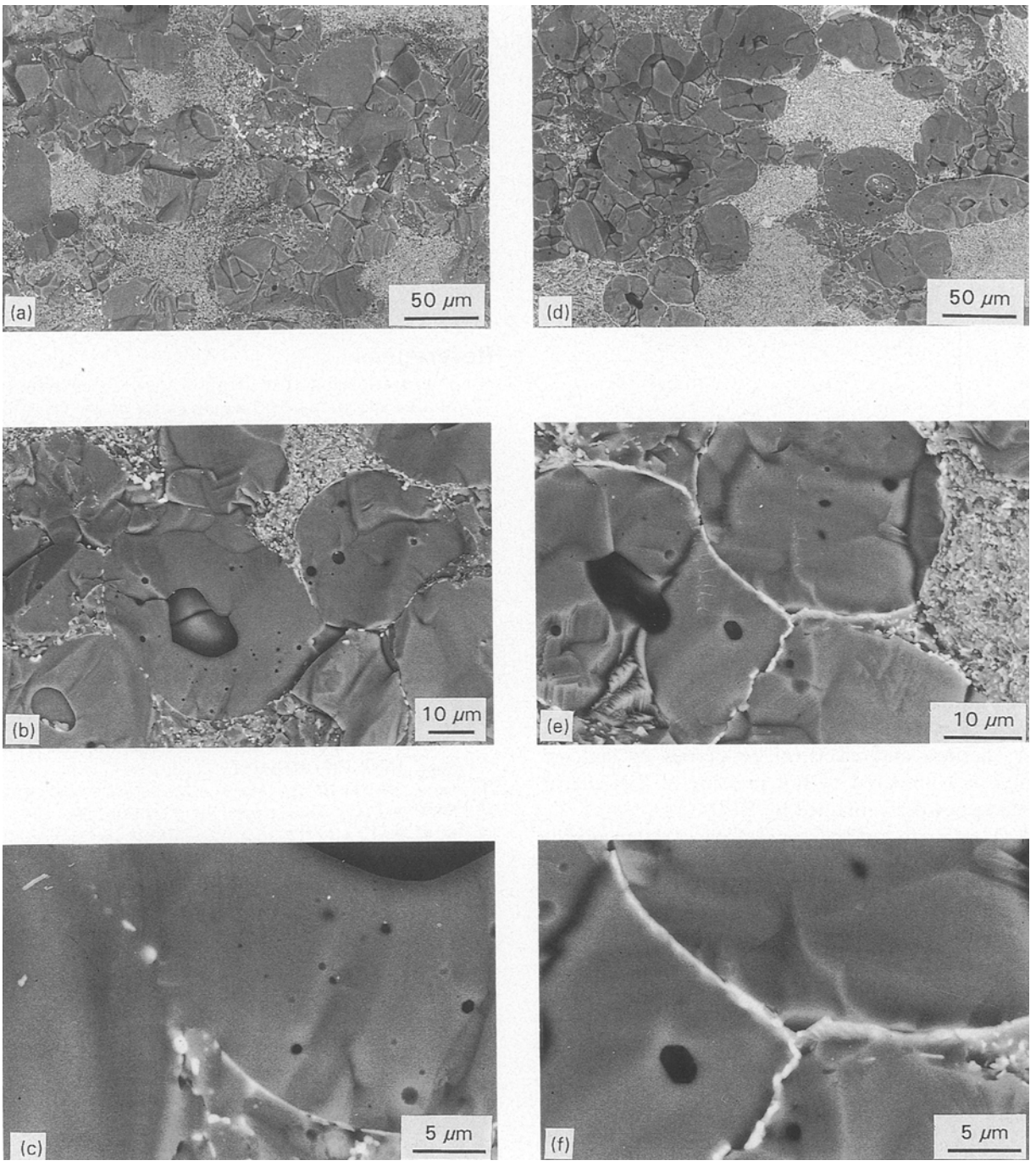

Figure 6 Back-scattered electron images of the fractured surface of hot-pressed specimens: (a–c) CVD-15, (d–f) CVD-90.

using a grain-boundary conduction model proposed by Tallan [12], the electrical resistivity was calculated as a function of TiN content for the present Al_2O_3–TiN composite system. The electrical resistivity of Al_2O_3 dispersant is much higher than that of the TiN matrix, and the total resistivity of the composite (ρ) is expressed by the equation

$$\rho = \rho_{TiN} \frac{K_c + \Phi}{K_c(1 - \Phi)}$$

where K_c is a shape factor of the dispersant grains and $K_c = 2$ in the present case of spherical Al_2O_3 particles; Φ is the volume fraction of Al_2O_3. Fig. 7 shows the calculated resistivity of the composite as a function of TiN content. The experimental values of measured resistivities are also plotted in the figure. A resistivity of 2×10^{-3} to 5×10^{-4} Ω cm is expected in the case of a composite with 2–6 vol % TiN. The measured value of resistivity in the CVD-90 specimen is a little higher than the calculated value, while the resistivity of the CVD-15 specimen is much higher than the expected value. It is suggested from the microstructure in Fig. 6 that a discontinuous TiN network may be responsible for the decrease in resistivity. The resistivities obtained in the present work are lower, however, than that (7.5×10^{-1} Ω cm) of the hot-pressed Al_2O_3–TiN (12.5 wt %) composite prepared by Kimura *et al.* [6], who estimate a lower connectivity of the TiN network.

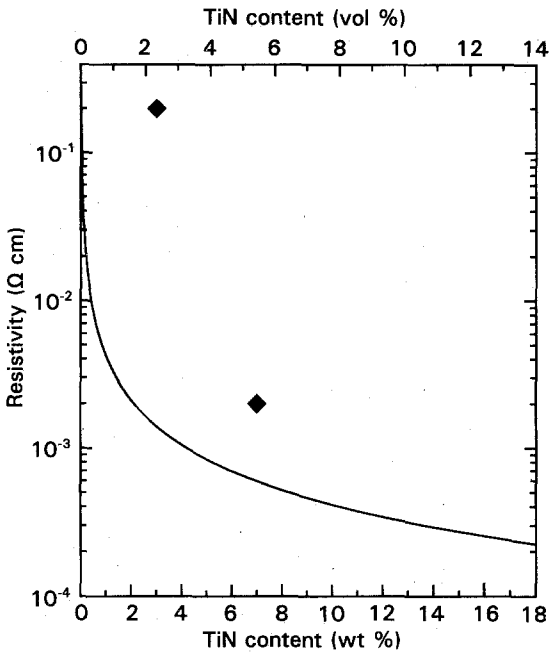

Figure 7 Resistivity of the Al_2O_3–TiN sintered composite as a function of TiN content: (——) calculated, (◆) measured.

4. Conclusions

The following conclusions were obtained by microstructural examination and evaluation of the mechanical, thermal and electrical properties of sintered composites prepared by hot pressing of TiN-coated alumina powders obtained by RPB-CVD.

1. A sintered composite in which titanium nitride was homogeneously distributed on the grain boundaries of Al_2O_3 grains was prepared by hot pressing of the TiN-coated alumina powder at 40 MPa and 1800 °C for 30 min.

2. The mechanical and thermal properties of the sintered composite depended on the composition and the microstructure. The mechanical strength and toughness were improved by addition of a small amount of TiN (3–7 wt %) to the grain boundaries of alumina ceramics.

3. The sintered composite showed electronic conductivity, having a resistivity of the order of 10^{-1} to 10^{-3} Ω cm. The electrical conduction was found to occur by grain boundary conduction through the TiN network in the composite.

References

1. R. P. WAHI and B. ILSCHNER, *J. Mater. Sci.* **15** (1980) 875.
2. M. LEE and M. P. BOROM, *Adv. Ceram. Mater.* **3** (1988) 38.
3. R. MATSUKI, H. UEDA, T. TAKENOUCHI, A. NAKAHIRA and K. NIIHARA, *Funtai-Oyobi-Funmatsu-Yakin (J. Jpn Soc. Powd. Powd. Metall.)* **38** (1991) 365.
4. A. NAKAHIRA, K. NIIHARA and T. HIRAI, *J. Ceram. Soc. Jpn* **94** (1986) 1986.
5. Y. W. KIM and J. G. LEE, *J. Mater. Sci.* **26** (1991) 1316.
6. I. KIMURA, N. HOTTA, K. ICHIYA and N. AITO, *J. Ceram. Soc. Jpn* **97** (1989) 1525.
7. H. ITOH, N. WATANABE and S. NAKA, *J. Mater. Sci.* **23** (1988) 43.
8. H. ITOH, K. HATTORI and S. NAKA, *ibid.* **24** (1989) 3643.
9. H. ITOH, K. HATTORI, M. OYA and S. NAKA, *J. Ceram. Soc. Jpn* **98** (1990) 499.
10. H. ITOH, H. SUGIMOTO, K. HATTORI and H. IWAHARA, *Funtai-Oyobi-Funmatsu-Yakin (J. Jpn Soc. Powd. Powd. Metall.)* **37** (1990) 1092.
11. D. S. McLACHLAN, M. BLASZKIEWICZ and R. E. NEWNHAM, *J. Amer. Ceram. Soc.* **73** (1990) 2187.
12. N. M. TALLAN, "Electrical Conductivity in Ceramics and Glass", Part B (Dekker, New York, 1978) p. 619.

Received 16 February
and accepted 3 June 1993